

Electrical and optical behaviour of vapour-grown SnS₂ crystals

S. K. ARORA, D. H. PATEL, M. K. AGARWAL

Department of Physics, Sardar Patel University, Vallabh Vidyanagar 388 120, Gujarat, India

Single-crystal growth of tin disulphide using chemical vapour (iodine) transport has been reported. The electrical resistivity, Hall mobility and optical absorption of the vapour-grown crystals have been investigated. The grown crystals show three different regions characterized by different operating conduction mechanisms. The electrical behaviour of the physical vapour-grown crystals in the 77–300 K temperature range reveals that the material can be obtained as a classical or a degenerate semiconductor depending upon the zone temperature interval. The optical absorption spectra in the 450–800 nm wavelength range has been analysed thoroughly to obtain direct and indirect allowed and forbidden transitions. An indirect transition assisted by phonon energy 0.04 eV has been identified in these crystals.

1. Introduction

The disulphides of the group IV elements, namely Ti, Zr, Hf and Sn, have remarkably similar properties, for example they are characterized by high metallic lustre, and they all crystallize in the CdI₂ structure consisting of a hexagonal close-packed sulphide lattice with metal atoms in alternate layers of the octahedral holes. An interesting feature of these layer compounds is that they can be crystallized as thin plates, a form very suitable for the investigation of optical and electrical properties and examination of structural defects. Within each layer the atoms are bound together by predominantly covalent forces as in the chalcogenides, or strongly ionic bonds as in the iodides. Each layer may be formed of three atomic planes X–M–X (CdI₂ structure), four planes X–M–M–X (e.g. Ga chalcogenides) or five layers X–M–X–M–X as for Bi₂Te₃ [1].

There have been a large number of studies on SnS₂ crystals grown by the chemical vapour transport (CVT) method in which iodine was the predominant transport agent used. The electrical resistivity [2] of the crystals has been reported to vary through orders of magnitude from 10² to 10¹² Ω cm, and the optical band gaps [3–8] to range from 2.12 to 2.44 eV. Our experience on vapour growth [9] indicates that the crystals grown using a transporting agent are highly contaminated and the growth conditions have a marked influence on the crystal properties. It is, therefore, of interest to attempt a detailed study of SnS₂ crystals grown by the physical vapour transport (PVT) method. The present paper describes the results on electrical, Hall mobility and optical properties of single crystals of SnS₂, grown using a two-zone muffle furnace fabricated in this laboratory. We have also examined SnS₂ single crystals grown by the chemical vapour transport method employing iodine as a transporter.

2. Experimental procedure

The growth of SnS₂ by PVT has already been reported elsewhere [10]. For their CVT, a quartz ampoule of size 23 cm × 2 cm was used. The tube was thoroughly cleaned by washing first with detergent soap solution, then kept immersed in aqua regia for 2–3 h and finally cleaned several times with double-distilled water. The ampoule was then filled with a stoichiometric composition of tin and sulphur (Johnson Matthey, UK, 99.99%) with traces of iodine, evacuated and sealed at a final pressure of 10⁻⁵ torr. The sealed ampoule was placed in a horizontal gradient two-zone muffle furnace. A temperature gradient of 600–670 °C was maintained for a growth period of 8 days including cooling intervals. The crystals obtained were invariably golden-coloured platelets of size 1 to 2 cm² in area and 20 to 100 μm in thickness.

The electrical and optical characteristics of the crystals were measured as described in the following section.

3. Results and discussion

3.1. Electrical behaviour

Electrical conductivity measurements were carried out in the temperature range 77–300 K, employing the conventional four-probe set-up. Four electrical contacts were made with evaporated indium on the (0001) cleavage face of each crystal and were arranged on a locally prepared sample holder which consists of a gold-plated copper assembly, mounted with a standard platinum thermometer (Pt 100) and a heater in close thermal contact.

SnS₂ was found to be a low-resistivity n-type crystal; $\rho = 3.7 \Omega \text{ cm}$ at room temperature (300 K) when the zone temperature gradient was 650–720 °C, but when the growth ampoule temperature was lowered to

580–640 °C, the room-temperature resistivity was found to have increased to $10^3 \Omega \text{ cm}$.

The electrical behaviour of the crystals grown by CVT was also examined in order to determine essentially the effect of the iodine transporter. The growth experiment yielded two kinds of crystal, one type having a resistivity of $10^4 \Omega \text{ cm}$ and the other of $50 \Omega \text{ cm}$ at 300 K.

The large deviation in the value of room-temperature resistivity on changing the furnace zone temperatures suggests that the crystals grown by PVT at 580–640 °C are different semiconductors to those grown at 650–720 °C, the former range giving crystals with an order of magnitude of higher resistivity than the latter range. In order to understand the distinct mechanisms of conduction operating in the two types of product, measurements of electrical resistivity were made at different temperatures (77–300 K) and the two plots thus obtained are shown in Fig. 1. Curve (a), showing a decrease of resistivity with increasing temperature, is characteristic of classical semiconductors, having activation energy $E_n = 0.24 \text{ eV}$, while curve (b) showing an increase of resistivity with increasing temperature is characteristic of degenerate semiconductors, having an activation energy $E_n = 0.01 \text{ eV}$ at relatively higher growth temperatures.

When the reaction between tin and sulphur takes place, aided by self-migration from the 720 °C zone to the 650 °C zone to form the crystals of SnS_2 , precipitation of the excess sulphur is likely to form extra energy states which in effect produce degeneracy in SnS_2 . Conduction in such materials is due to lattice scattering rather than carrier activation as the predominant factor to influence resistivity. The excess donor states introduced by even the slightest deviation from stoichiometry lie close to the conduction band edge

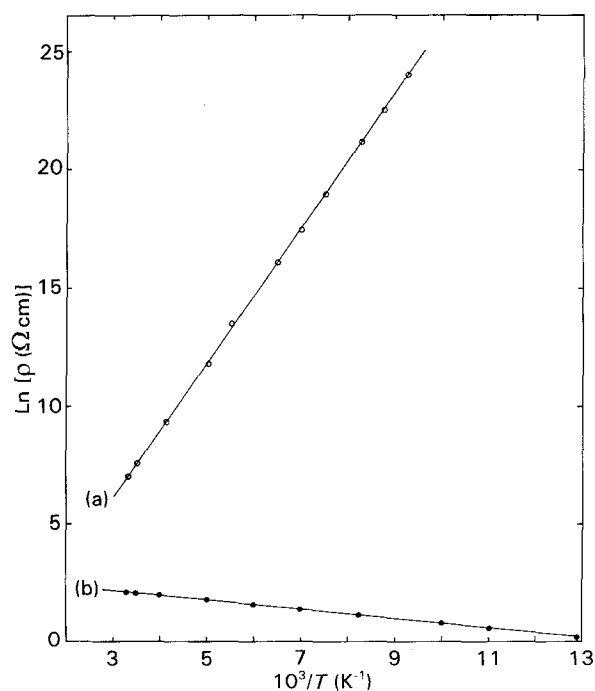


Figure 1 Resistivity as a function of temperature for SnS_2 crystals grown by physical vapour transport, with different charge growth gradients: (a) 580–640 °C, (b) 650–720 °C.

and are ionized more at higher temperatures, entailing continuously enhanced conductivity with activation energy $E_n = 0.01 \text{ eV}$ (curve (b) in Fig. 1) as observed. This kind of degeneracy in vapour-grown SnS_2 crystals has also been reported by Kourtakis *et al.* [11].

On the other hand, SnS_2 crystals grown by iodine vapour transport (600–670 °C) show a different behaviour of resistivity versus temperature, as shown in Fig. 2. As one might expect, the material exhibits a classical semiconducting behaviour, revealing a three-step activation process of conduction. Region III, showing a greater resistivity change $\Delta\rho$, has a greater value of activation energy compared to the regions I and II (Table I). Interestingly, the crystals grown in a single ampoule have been found to show resistivity values varying from 50 to $10^4 \Omega \text{ cm}$, the higher-resistivity crystals being those harvested from the cold end, while the lower-resistivity crop grew near the middle of the ampoule. This observation is in contrast to those of Said and Lee [2] but similar to those of Ishizawa and Fujiki [12]. In our case, the varying minute traces of iodine inclusion during transport from 670 to 600 °C might be thought of as the source of varying resistivity.

It is interesting to note that the three distinct regions can be shown to obey an equation of the form

$$\rho = \rho_0 \exp(E_n/kT) \quad (1)$$

For the sample chosen, the computed values of ρ_0 and E_n are given in Table I.

3.2. Hall measurements

Samples whose ohmic contacts were checked before measurements were inserted into the bore of an elec-

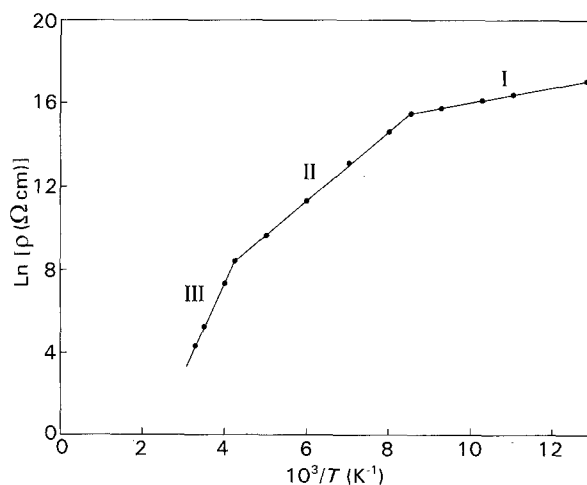


Figure 2 Resistivity as a function of temperature for SnS_2 crystals grown by chemical vapour transport, showing regions I, II and III.

TABLE I Values of activation energy and pre-exponential factor for CVT SnS_2 single crystals

Region I	Region II	Region III
$\rho_{0I} = 2.68 \times 10^5$	$\rho_{0II} = 4.2631$	$\rho_{0III} = 4.53 \times 10^{-5}$
$E_I = 0.03 \text{ eV}$	$E_{II} = 0.14 \text{ eV}$	$E_{III} = 0.37 \text{ eV}$

tromagnet. The Hall mobility μ_H and carrier concentration η were then measured in air at room temperature (300 K). The data obtained (Table II) on our SnS_2 crystals are in fair agreement with those obtained by previous workers [11–14].

3.3. Optical behaviour

Optical absorption spectra of the grown SnS_2 crystals were obtained with a double-beam spectrophotometer (Shimadzu UV-VIS spectra UV-2100) in the wavelength range 450–800 nm at room temperature. The single crystal, mounted on a clean quartz slide, was placed in the beam path in such a way that its c plane was perpendicular to the direction of the indirect beam. The percentage transmittance recorded as a function of incident wavelength for the (0001) face of the crystal is shown in Fig. 3. The optical absorption data were analysed in terms of the theory of Bardeen *et al.* [15] which gives for an indirect transition

$$\alpha = \frac{B}{h\nu} (h\nu - E_g)^r \quad (2)$$

where E_g is the indirect band gap and $h\nu$ the photon energy. If $r = 2$, the transition is allowed and for $r = 3$, the transition is forbidden.

The graphical relationships between energy and $(\alpha h\nu)^{1/2}$ and $(\alpha h\nu)^{1/3}$ are shown in Fig. 4. The energy intercept gives indirect allowed and forbidden band gaps of 2.12 and 2.07 eV, respectively. These values are in good agreement with those of Gupta *et al.* [4] and Domingo *et al.* [6], respectively.

Based on the theory of interband optical absorption, the electronic transition near the fundamental absorption edge may be analysed [16] by considering the plot of α^n versus $h\nu$, according to the equation.

$$\alpha^n = A_k (h\nu - E_{gi}), \quad (3)$$

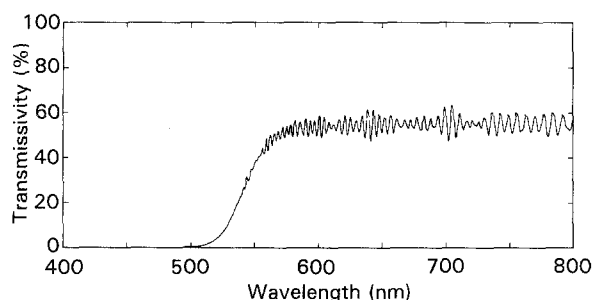


Figure 3 Optical transmission spectra for single-crystal SnS_2 at 300 K.

TABLE II Electrical transport parameters determined at room temperature (300 K) on vapour-grown SnS_2 single crystals

Growth process	Resistivity at 300 K ρ (Ωcm)	Mobility μ_H ($\text{cm}^2 \text{V}^{-1} \text{s}^{-1}$)	Carrier concentration η (cm^{-3})	Activation energy (eV)	Carrier type
PVT					
650–720 °C	3.7	4.3	3.92×10^{17}	0.01	n
580–640 °C	10^3	5.6	10^{15}	0.24	n
CVT (I_2)					
600–670 °C	$50\text{--}10^4$	4.5	2.31×10^{16}	0.37, 0.14, 0.03	n

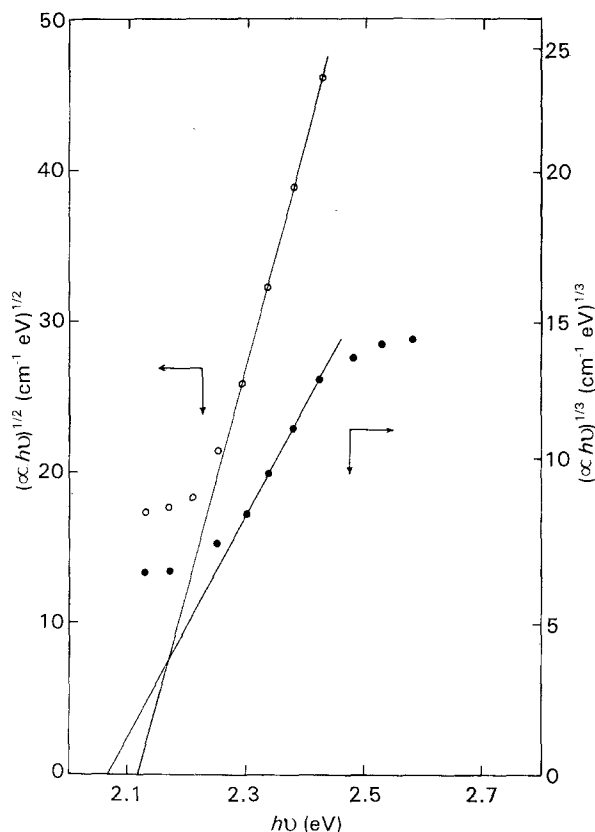


Figure 4 Plots of $(\alpha h\nu)^{1/2}$ and $(\alpha h\nu)^{1/3}$ versus photon energy.

where A_k is a constant and $n = 2, 1/2$ for the allowed and $n = 2/3, 1/3$ for the forbidden direct and indirect transitions, respectively. Analysis of the three straight lines of $\alpha^{1/2}$ versus $h\nu$ in Fig. 5 has been used to separate the individual contributions of the phonons. The partial absorption coefficient α_1 is found by extrapolating the first dotted segment marked 1; second, the total absorption coefficient $\alpha = (\alpha_1 + \alpha_2)$ is obtained corresponding to $h\nu$ values in the segment CB, and then α_1 is subtracted from α to get $(\alpha - \alpha_1)^{1/2}$, thus resulting in curve (a) of Fig. 6. Then, taking the segment CB marked 2 to give α_2 , it is subtracted from the total α obtained from another set of $h\nu$ values chosen from the next segment BA. Obviously this gives $(\alpha - \alpha_2)^{1/2} = \alpha_3^{1/2}$ and thus the curve (b) of Fig. 6 is obtained. One gets the two different fitted energy gaps listed in Table III and estimated threshold values given by

$$\begin{aligned} (h\nu_{\text{thr}})_a &= E_g - E_p \\ (h\nu_{\text{thr}})_e &= E_g + E_p \end{aligned} \quad (4)$$

where $(h\nu_{\text{thr}})_a$ and $(h\nu_{\text{thr}})_e$ are the threshold photon energies for absorption and emission, respectively.

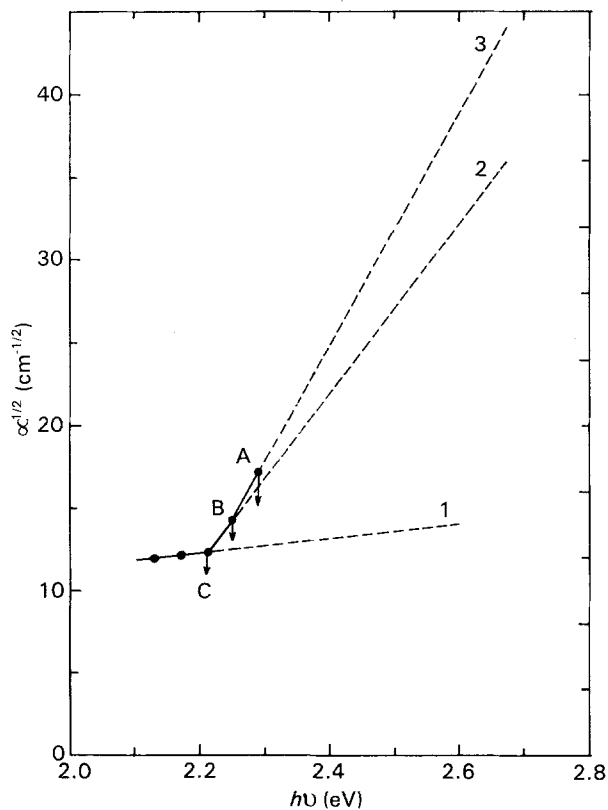


Figure 5 Plot of $\alpha^{1/2}$ versus photon energy.

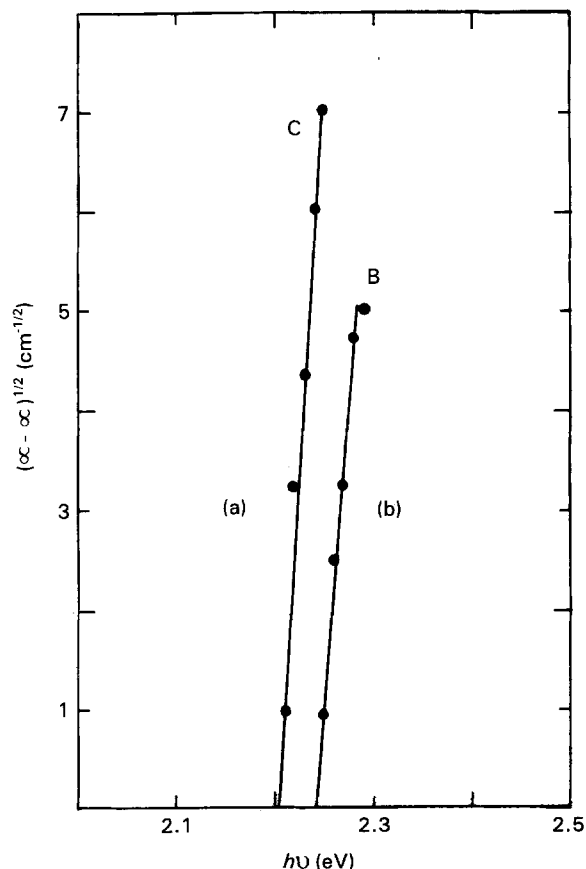


Figure 6 Plot of $(\alpha - \alpha_1)^{1/2}$ versus photon energy.

The evaluation of the values of A_k (given in Table III) for the three segments has been carried out using the equation

$$A_k = \frac{\alpha_i}{h\nu - E_{gi}} \quad i = 2, 3; k = 1, 2 \quad (5)$$

TABLE III Values of fitted and estimated/threshold E_g and A parameters

No.	Fitted E_g (eV)	A_k ($\text{cm}^{-1} \text{eV}^{-2}$)	Knee point	Estimated threshold E_g (eV)
1	2.24	11.616×10^3	B	2.25
2	2.205	6.604×10^3	C	2.21

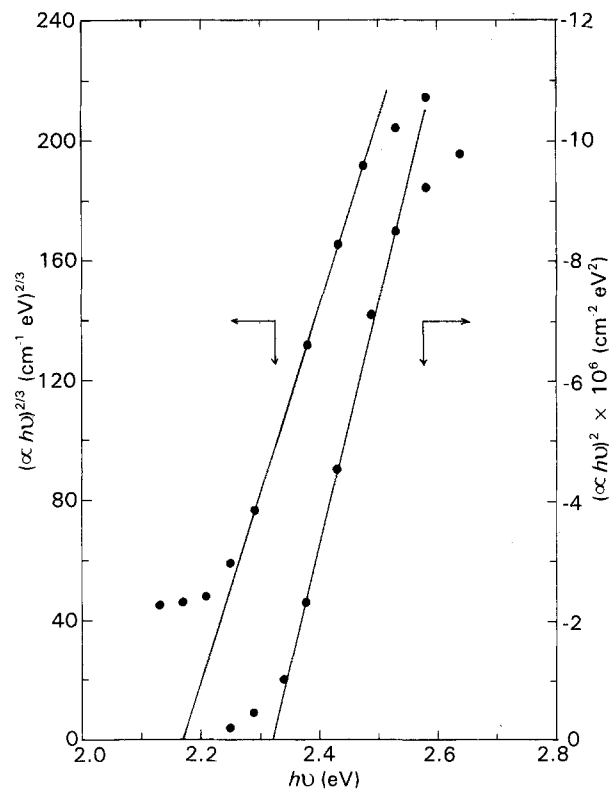


Figure 7 Plots of $(\alpha h\nu)^{2/3}$ and $(\alpha h\nu)^2$ versus photon energy.

Thus the threshold energy interval of 0.04 eV represents the lattice phonon contribution involved in the indirect transitions in SnS_2 crystals. This value, which corresponds to $\bar{\nu} = 321 \text{ cm}^{-1}$, is in fair agreement with the theoretically predicted and experimentally demonstrated values of LO phonons in the $\text{SnS}_x\text{Se}_{2-x}$ ($0 \leq x \leq 2$) crystals studied by Gupta *et al.* [17].

Finally, the plots of $(\alpha h\nu)^{2/3}$ and $(\alpha h\nu)^2$ versus $h\nu$ in Fig. 7 have been used to give the allowed direct and forbidden energy gaps to be 2.32 and 2.17 eV, respectively, as obtained by the intercept of extrapolated zero absorption coefficient. Evidently, one is led to conjecture that in the region of higher photon energy, a direct transition in SnS_2 crystals prevails.

References

1. P. A. LEE, G. SAID, R. DAVIS and T. H. LIM, *J. Phys. Chem. Solids* **30** (1969) 2719.
2. G. SAID and P. A. LEE, *Phys. Status Solidi (a)* **15** (1973) 99.
3. J. GEORGE and C. K. VALSALA KUMARI, *J. Cryst. Growth* **63** (1983) 233.
4. V. P. GUPTA, P. AGARWAL, A. GUPTA and V. K. SRIVASTAVA, *J. Phys. Chem. Solids* **43** (1982) 291.
5. D. L. GREENWAY and R. NITSCHKE, *ibid.*, **26** (1965) 1445.
6. G. DOMINGO, R. S. ITOGA and C. R. KANNEWURK, *Phys. Rev.* **193** (1966) 536.

7. M. J. POWELL, *J. Phys. C. Solid State Phys.* **10** (1977) 2967.
8. T. SHIBATA, N. KAMBE, Y. MURANUSHI, T. MIURA and T. KISHI, *J. Phys. D. Appl. Phys.* **23** (1990) 719.
9. A. ARUCHAMY and M. K. AGARWAL, in "Photoelectrochemistry and Photovoltaics of Layered semiconductors", edited by A. Aruchamy (Kluwer, Dordrecht, USA, 1992) pp. 319
10. S. K. ARORA, D. H. PATEL and M. K. AGARWAL, *J. Cryst. Growth* **131** (1993) 268–327
11. K. KOURTAKIS, J. DICARLO, R. KERSHAW, K. DWIGHT and A. WOLD, *J. Solid State Chem.* **76** (1988) 186.
12. Y. ISHIZAWA and Y. FUJIKI, *J. Phys. Soc. Jpn* **35** (1973) 1259.
13. T. SHIBATA, Y. MURANUSHI, T. MIURA and T. KISHI, *J. Phys. Chem. Solids* **52** (1991) 551.
14. B. FOTOUHI and A. KATTY, *Electrochim. Acta* **32** (1987) 1149.
15. J. BARDEEN, F. J. BLATT and L. H. HALL, in Proceedings of Photoconductivity Conference, Atlantic City, NJ (Wiley, New York, 1956) p. 146.
16. S. K. ARORA, T. MATHEW and N. M. BATRA, *J. Phys. Chem. Solids* **50** (1989) 665.
17. H. C. GUPTA, G. SOOD, M. M. SINHA and B. B. TRIPATHI, *Phys. Rev. B.* **37** (1988) 14.

Received 5 August 1993

and accepted 19 January 1994